

PACS numbers: 42.65.–k; 78.67.Hc; 79.20.Ws
DOI: 10.1070/QE2015v045n12ABEH015909

Optical power limiting in ensembles of colloidal Ag_2S quantum dots

O.V. Ovchinnikov, M.S. Smirnov, A.S. Perepelitsa, T.S. Shatskikh, B.I. Shapiro

Abstract. **The effect of power limiting for optical radiation at a wavelength of 660 nm with a pulse duration of 10 ms and operation threshold of 2.2–3.1 mJ cm^{-2} is observed in ensembles of colloidal Ag_2S quantum dots (QDs). Using the *z*-scanning method in an open-aperture scheme it is found that the power is limited mainly due to reverse saturable absorption caused by two-photon optical transitions that involve energy levels of Ag_2S photoluminescence centres, related to structural impurity defects in colloidal Ag_2S QDs. At the same time, the *z*-scanning in a closed-aperture scheme demonstrates the formation of a thermal dynamic lens.**

Keywords: *power limiting, inverse-saturation absorption, colloidal quantum dots, silver sulphide.*

1. Introduction

The progress of photonics and related technologies determines the great interest in the design of the systems that control the optical radiation parameters [1–25]. Thus, high-efficiency optical power limiters provide the protection of human vision organs (in the spectral range 350–700 nm the threshold of irreversible damage is 2.5 mJ cm^{-2}, the pulse duration being not smaller than 0.25 s) [3]. They also protect optical instruments and devices (photoelectronic multipliers, photodiodes, etc.), equalise the intensities of light flows in fibre optical systems of data transmission and processing, etc. [1–10]. Passive methods of optical power limiting that require creation of smart materials, capable of controlling the radiation intensity, are particularly promising.

Nanomaterials and composites based on them are a relatively new class of media, in which the effect of optical power limiting can be implemented [6–14]. This effect and the mechanisms responsible for it are studied mainly in carbon nanomaterials [1, 2, 4–7], in complexes based on metallic silver and gold particles [7–13], as well as in nanostructures based on silicon and its compounds [1, 7, 13–15]. As a rule, the nonlinear optical properties of gold and silver nanoparticles are investigated in suspensions, various dielectric matrices, thin films, glasses, as well as for particles coated with protective shells (core–shell nanostructures). In such materials, the laser radiation power limiting was observed at the wavelengths 532 and 1064 nm at the intensity 1–1.5 J cm^{-2} and the pulses duration from 30 fs to 10 ns [7].

Considerable reduction of the limiting threshold can be achieved using semiconductor crystals with localised states [17–25]. Targeted formation of localised states with given parameters provides the possibility of one- and two-photon impurity transitions [25–31]. They can lead to optical nonlinearities of the inverse-saturation absorption type, to nonlinear refraction, etc. [1, 25]. However, in the case of semiconductor crystals and thin monocrystalline films the difficulties arise in achieving the required concentration of the localised states with the appropriate energy properties. On the other hand, the use of polycrystalline samples is not attractive because of their insufficient linear transmission reduced by light scattering.

Colloidal solutions, containing semiconductor nanocrystals, are promising because of the possibility to achieve optical homogeneity of the limiting layer. Up to date, there are a few papers devoted to the analysis of the optical power limiting efficiency in colloidal solutions, containing semiconductor nanocrystals or quantum dots (QDs) of CdS, PbS, ZnSe, Ag_2S, CdSe, AgCl(I), etc. [9–11, 14, 18, 25, 32–40], as well as nanocomposites based on them [41–43]. Thus, in Ag_2S–CdS nanoparticles with the average size ~10 nm [41] the power limiting was observed for the laser radiation with the energy density up to 1.8 J cm^{-2} and the wavelength λ = 532 nm, the pulses duration being from 25 ps to 7 ns and the repetition rate being 10 Hz. The optical nonlinearities, responsible for this effect, are due to the two-photon absorption of light, as well as to the light absorption by free charge carriers. For semiconductor QDs the simultaneous manifestation of several types of optical nonlinearity is often observed [35, 36, 40–42]. However, the influence of the localised states on them is discussed insufficiently. Only some studies are known, carried out in semiconductor monocrystals [17, 37]. Still poorly studied is the relation between the quantum size effects in semiconductor QDs with the optical nonlinearities, giving rise to power limiting. At present, there are difficulties in constructing models, relevant to the experiment and allowing for the influence of the quantum confinement on the energetics of the localised states.

One of the interesting materials for low-threshold power limiting in the visible and near-IR spectral ranges are Ag_2S QDs [9, 10, 12]. The optical radiation power limiting effect in such QDs is discussed in a number of papers [9, 10, 12, 39, 40]. Most of them are devoted to the optical limiting effects for the laser pulses with the duration 5–15 ns (λ = 532 nm), the energy density being $6.5–1.8 \times 10^3$ mJ cm^{-2}. There is evidence

O.V. Ovchinnikov, M.S. Smirnov, A.S. Perepelitsa, T.S. Shatskikh
Voronezh State University, Universitetskaya pl. 1, 394006 Voronezh, Russia; e-mail: Ovchinnikov_O_V@rambler.ru, opt@phys.vsu.ru, a-perepelitsa@yandex.ru;
B.I. Shapiro M.V. Lomonosov Moscow State University of Fine Chemical Technologies, prosp. Vernadskogo 86, 119571 Moscow, Russia

Received 27 July 2015
Kvantovaya Elektronika **45** (12) 1143–1150 (2015)
Translated by V.L. Derbov

of simultaneous manifestation of a number of optical nonlinearities leading to power limiting (the absorption by free charge carriers [10], the nonlinear refraction, the nonlinear scattering, the two-photon absorption [39] and the formation of a thermally induced dynamic lens [40]). It is worth paying attention to the fact that the role of the localised states, the concentration of which is high in such a nonstoichiometric compound as Ag_2S [44–46], in the optical power limiting in colloidal Ag_2S QDs is not discussed. At the same time, the small width of the bandgap in Ag_2S mono- and polycrystals (0.9–1.0 eV) [43, 47] allows the control of the position of the optical absorption spectrum within the wavelength range 1100–350 nm at the expense of the quantum size effect. The possibility of laser power limiting at the wavelengths beyond the optical absorption edge from the long-wavelength side also appears. The technological methods of preparing Ag_2S QDs with variable ensemble parameters and linear optical properties are already known [46–54].

This paper reports the study of the power limiting effect involving the structural impurity defects in ensembles of colloidal Ag_2S QDs, occurring for the radiation with λ = 660 nm and the maximal laser radiation flux density 1.2 W cm^{-2}, which corresponds to the energy density per pulse 12 mJ cm^{-2} for the pulse duration of 10 ms.

2. Samples under study

The studied samples were ensembles of colloidal Ag_2S QDs with the average size 1.7–3.7 nm, dispersed in gelatine. Their synthesis was implemented by pouring together two streams of aqueous solutions of the initial reagents $AgNO_3$ and Na_2S with a peristaltic pump into a temperature-controlled reactor, containing the 2% solution of inert photographic gelatine at 70 °C. The description of the synthesis technique is presented in Refs [46, 55]. The resultant sols were subject to thermal treatment at 90 °C and permanent stirring in the reactor during 3 h. The thermal treatment of the colloidal QDs of Ag_2D reduced the particle size dispersion at the expense of recrystallization caused by the Ostwald ripening (small QDs are dissolved due to a larger curvature of the surface in correspondence with the Gibbs–Thomson effect, while the large ones somewhat increase their size) [56]. Besides reducing the size dispersion, the recrystallization can also lead to the change in the crystal structure defects concentration, first of all, near the interfaces of the nanoparticles.

By changing the quantity of the initial reagents, we achieved the formation of the ensembles of Ag_2S QDs having different size. The choice of the amount and proportion of the reagents was based on the data of Refs [48–54], where the values close to the optimal ones were found. As a result of the synthesis we obtained the samples with the QDs-to-gelatine mass ratio 2.1×10^{-2} (sample 1) and 1.1×10^{-1} (sample 2). Samples 1′ and 2′ differed from Samples 1 and 2 by the thermal treatment at 90 °C.

The analysis of X-ray diffraction (XRD) patterns, recorded using an ARL X'TRA diffractometer (Switzerland) at the $K_{\alpha 1}$ line of copper radiation, has shown that the synthesised particles of Ag_2S are crystalline structures with a monocline lattice. The size of the colloidal QDs was measured using a Libra 120 transmission electron microscope (TEM) (Carl Zeiss, Germany). The analysis of TEM data has shown that the mean size of the colloidal Ag_2S QDs in the ensemble amounted to 1.7 ± 0.2 and 3.0 ± 0.2 nm for samples 1 and 2, respectively [Fig. 1b, histograms (*1*) and (*2*)]. The considerable dispersion of sizes, amounting to 35%–45%, is due to the chosen approach to the synthesis of QDs of Ag_2S in the aqueous solution of the polymer [53, 57].

The thermal treatment of the sample series at 90 °C provided a reduction of size dispersion by 5%–15% and an increase in the Ag_2S QD mean size by 0.7–0.8 nm [Fig. 1b, histograms (*1′*) and (*2′*)]. For sample 1′ the mean particle size was 2.5 ± 0.2 nm, and for sample 2′ it was 3.7 ± 0.2 nm.

3. Optical study techniques

The spectral properties of the synthesised samples were analysed from the point of view of linear transmission, spectral position and intensity of the intrinsic and impurity absorption of light, and luminescence. We recorded the spectra of the Ag_2S QDs optical absorption using a USB2000+ spectrophotometer with a USB-DT radiation source (Ocean Optics, USA). The luminescence properties of the colloidal QDs were studied by means of an automated spectral system based on a MDR-23 diffraction monochromator (LOMO, Russia). As a

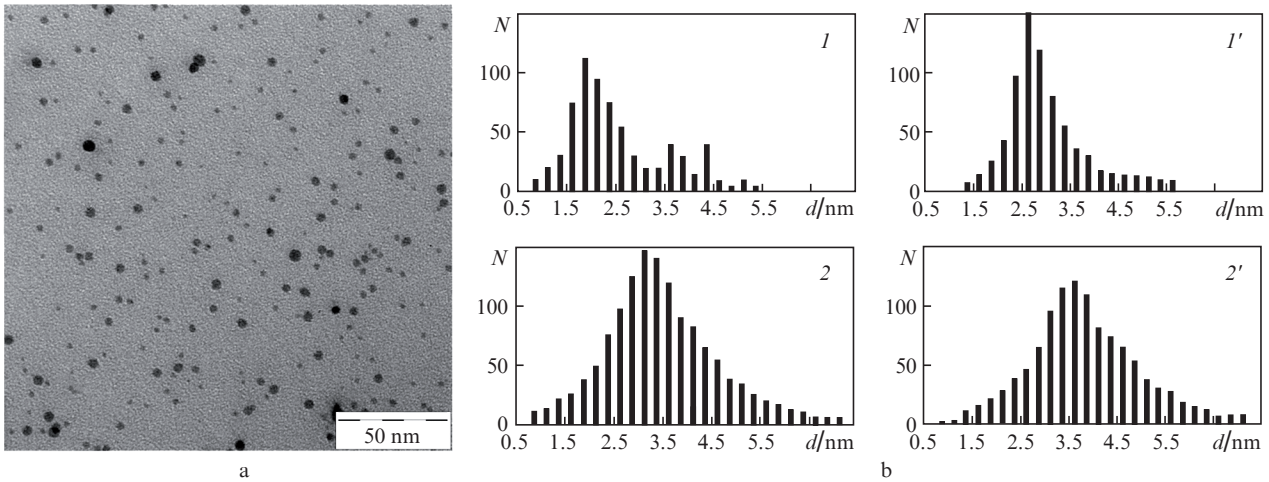

Figure 1. TEM images of colloidal Ag_2S QDs: (a) sample 1 and (b) histograms of their size distributions (the histogram numbers *1*, *1′*, *2* and *2′* correspond to the sample numbers); *N* is the number of particles.

photodetector for the near-IR range, we used a high-stability low-noise PDF10C/M photodiode (Thorlabs Inc., USA) with an incorporated amplifier. The system operation was controlled automatically using a Celeron-433 PC equipped with the interface unit. The photoluminescence excitation sources were LCD PLTB450 laser diodes (Osram, Germany), providing the radiation at the wavelength 440 nm and LPC-826 laser diodes (Mitsubishi, Japan), radiating at the wavelength 660 nm.

To study optical nonlinearities, we used the *z*-scanning method [58–60]. We measured the dependence of the normalised transmission in the sample, placed after a focusing lens, on the distance between the focal plane of the lens and the sample (below referred to as *z*-scan) [58, 59]. The measurement of this dependence allows the determination of the dominant mechanism of the optical nonlinearity [25, 58–60]. Thus, in the case of two-photon absorption or inverse-saturation absorption in the sample the *z*-scan is symmetric with respect to the focal plane. If the refractive index in the sample is changed (nonlinear refraction), then a focusing of defocusing dynamic lens arises in it. In this case the *z*-scan curve becomes asymmetric and acquires a minimum before the focal plane and a maximum after it, or vice versa, depending on the sign of the refractive index [25, 58–60].

The analysis of the power limiting and the physical mechanisms of optical nonlinearity was performed using the *z*-scanning experimental setup in the configurations with both the closed aperture (the scheme is presented in Fig. 2) and the open one. The source of radiation was the LPC-826 laser diode with $\lambda = 660$ nm and power 230 mW. The rotating chopper produced the pulses with the duration 10 ms and the pulse repetition rate 720 ms. The light passing through the lens with the focal length 15 cm was focused on the sample fixed in a holder. The diameter of the laser beam waist amounted to 22 μm. The radiation passed through the sample was detected by an FDS10X10 silicon photodiode (Thorlabs, USA), placed behind the limiting aperture at the distance of 50 cm from the lens focus and operating in the regime of measuring the photocurrent (closed aperture scheme). In the course of the open-aperture studies, the limiting aperture was removed from the setup scheme, and the photodiode was placed at the distance of 10 cm from the lens focus. In this case, all radiation, transmitted through the sample, was recorded by the photodetector. To study the effect of optical radiation power limiting, the holder with the sample was placed in the lens focus. The linear dependence of the photocurrent arising in the photodiode on the intensity of the incident radiation was checked by means of NS-6–NS-12 neutral optical filters. The signals were recorded using a DC1102C storage oscilloscope (Rigol, China).

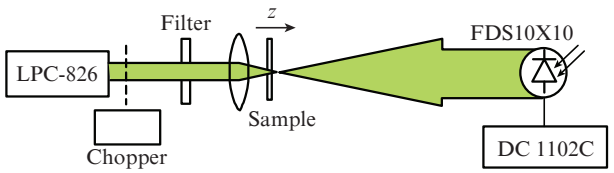

Figure 2. Schematic diagram of the setup implementing the *z*-scanning method.

4. Spectral properties of colloidal Ag_2S QDs

The samples of ensembles of colloidal Ag_2S QDs possess size-dependent spectral properties. They are characterised by broad absorption bands in the region 2.5–4.0 eV (Fig. 3a). In most cases, the absorption bands had the singularities in the region 2.80–2.90 eV [46, 49], characteristic for the exciton transitions in QDs. The blurring of the sharp exciton maximum is probably due to the existing dispersion of QD sizes within each of the studied ensembles [51–53]. At the same time, in the long-wavelength part of the optical absorption spectrum (1.6–2.5 eV) a considerable optical density was observed. The main reasons are supposed to be the size dispersion in the ensemble of Ag_2S QDs and the absorption of light by the impurity states. The essential effect of the non-stoichiometric nature of the monoclinic phase of the Ag_2S compound (sometimes $Ag_{2-x}S$) manifests itself in the significant concentration of crystal structure defects [41, 46] that play the role of localised states, some of them being radiative recombination centres.

These structure impurity defects manifest themselves in photoluminescence, excited at the temperature 300 K by the radiation with $\lambda = 440$ nm (2.8 eV) that corresponds to the singularity in the absorption band. The photoluminescence

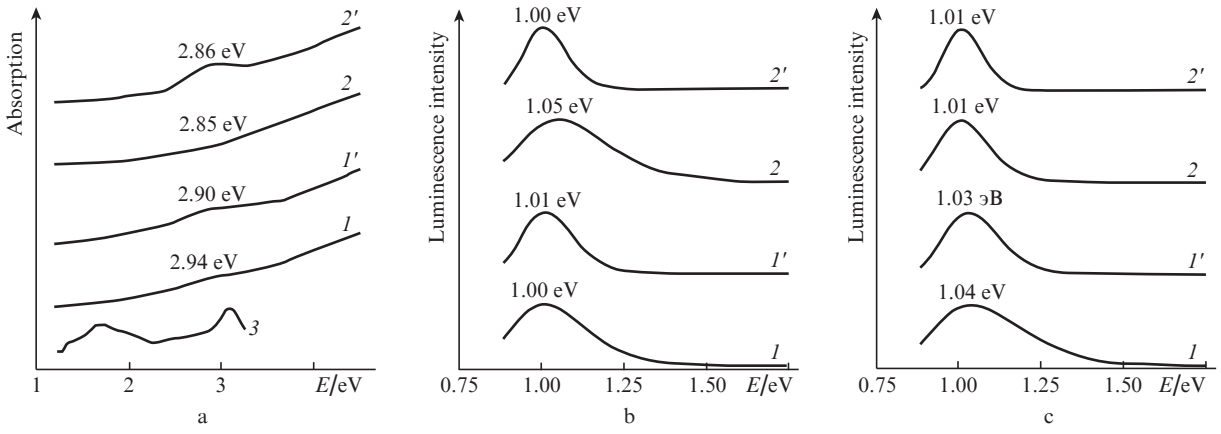

Figure 3. Optical absorption spectra (a) and normalised luminescence spectra of the samples of colloidal Ag_2S QD ensembles excited by the radiation with the wavelengths (b) 440 and (c) 660 nm. The numbers of curves correspond to the numbers of the samples; curve (*3*) is the spectrum of photoexcitation of Ag_2S QDs of sample 2′.

spectra are bands with the maxima at 1.00–1.05 eV and the half-maximum half-width 0.12–0.26 eV (Fig. 3b). The significant Stokes shift of the luminescence band and its half-width indicate the recombination nature of the observed luminescence of the colloidal Ag_2S QDs.

For the studied samples we demonstrated the possibility of exciting the IR luminescence by the radiation with λ = 660 nm (1.88 eV) (Fig. 3c). This observation is not incidental. For the QDs of Ag_2S a wide spectrum of photoluminescence excitation was found [Fig. 3a, curve (*3*)], expanding from the region of exciton absorption to the band of photoluminescence. In these spectra the maxima were observed in the region 3.0 eV and 1.5–1.7 eV. The band with the maximum near 3.0 eV is located in the region of exciton absorption. In its turn, the capture of electrons and holes by the localised states in QDs leads to the appearance of recombination luminescence. The existence of a long-wavelength band in the luminescence excitation spectrum in the region of 1.3–2.0 eV means the high probability of optical transitions from the energy levels of luminescence centres to the energy levels of size quantisation of electrons (holes). In this case, the optical transitions that determine the process of exciting the luminescence centres are expected to occur with the participation of highly excited size quantisation energy levels, thus forming the observed spectrum of luminescence excitation [Fig. 3a, curve (*3*)].

We should note that the efficiency of two-quantum excitation of luminescence via virtual states for the used exciting light fluxes (the density smaller than 0.1 W cm^{-2}) is insignificant. Indeed, the estimated number of quanta absorbed per unit time by a single QD with the size 1.7 nm and the absorption coefficient $\sim 10^3$ cm^{-1} is $\sim$7 quanta per second. Since the lifetime of the charge carriers in the excited state amounts to microseconds and sometimes even nanoseconds [61, 62], the above observations convince us of the possibility of direct excitation of the luminescence centres.

The change in the conditions of the sample synthesis, consisting in their thermal treatment at 90 °C, leads to the segregation of a peak caused by exciton transitions in the spectrum of optical absorption [Fig. 3a, curves (*1′*) and (*2′*)]. For sample 2′ we observed the formation of a distinct maximum in the region 2.8 eV, where in the absorption spectrum of sample 2 one could hardly see a small singularity. These measurements agree with the reduction of particle size dispersion by 5%–15%, determined from TEM images.

5. Effect of optical radiation power limiting

Thus, in the studied ensembles of Ag_2S QDs we found the existence of the spectral region of impurity absorption that may be the due to IR photoluminescence centres, possessing the property of direct excitation by the quanta with the energy smaller than that of an exciton. The presence of states with such properties leads to a multiple increase of the efficiency of two-quantum transitions, when using weak light fluxes (10^{-10}–10^{-3} W cm^{-2}) to excite the anti-Stokes luminescence, for which it is known that the dependence of the glow intensity on the intensity of excitation is nonlinear [25–31]. On the other hand, the threshold of the optical radiation power limiting due to the impurity transitions via real localised states becomes considerably reduced [5, 15, 17, 25, 37].

In the studied Ag_2S QDs the effect of power limiting was observed using the optical radiation with λ = 660 nm, the energy density of laser pulses up to 12 mJ cm^{-2}, and the pulse duration 10 ms. Note that due to the presence of a focusing lens the energy density at the sample, located in the beam waist region, appears to be much higher and approaches 600 J cm^{-2}.

The samples were located in the lens focus (see Fig. 2). The dependences presented in Fig. 4 demonstrate the effect of optical power limiting, i.e., the reduction of transmission under the increase in the radiation intensity. The operation threshold for the input radiation amounted to 3.1 ± 0.2 mW cm^{-2} for the Ag_2S QDs with the mean size 1.7 nm and 2.8 ± 0.2 mW cm^{-2} for the Ag_2S QDs with the mean size 3.0 nm. With the growth of the mean QD size in the ensemble from 1.7 to 3.0 nm we observed the reduction of the deviation of the experimental curves from those of linear transmission at the pulse energy density 5.69 mJ cm^{-2}, which corresponds to the fall of the efficiency of the optical radiation power limiter.

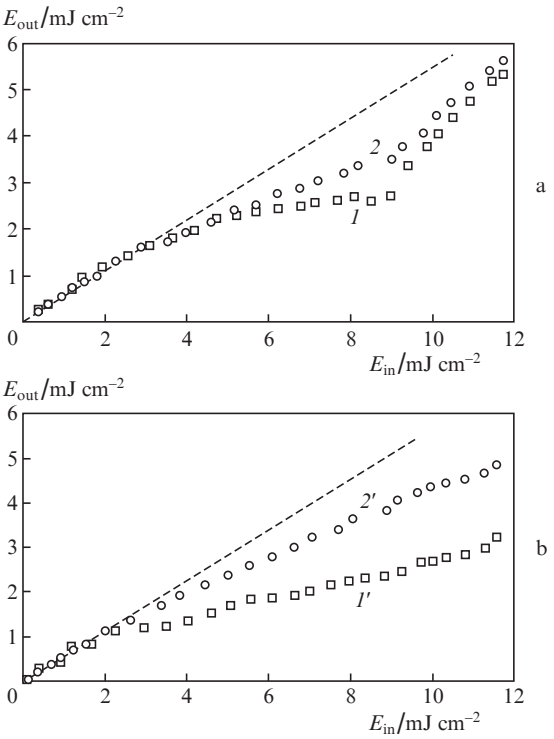

Figure 4. Dependences of the energy density of optical radiation transmitted through the sample on the energy density of the incident optical radiation for (a) samples *1* and *2* and (b) samples *1′* and *2′*. The dashed lines indicate the level of linear transmission of the studied samples. The curve numbers correspond to the sample numbers.

This property can be due to several factors. First, when the QD size increases, the surface-to-volume ratio decreases. If the power limiting is due to surface effects, the observed behaviour will be just of this kind. Second, with the growth of the QD size the effective cross section of the absorption by defects can also change, which will lead to the limiting efficiency change.

As noted in a number of papers, for pulses of micro- and millisecond duration the power limiting process becomes strongly affected by the recombination and diffusion of charge carriers, as well as the heat diffusion from the region of maximal radiation intensity in the sample [5, 17, 37]. We will discuss these effects in the next Section in more detail.

Starting from the incident radiation energy density 9 mJ cm^{-2}, we observed the change in the character of the experimental dependence [Fig. 4a, curves (*1*) and (*2*)], namely, the transmission level grows, i.e., the sample becomes clearer. Thus, the dynamic range of the optical radiation power limiting in samples 1 and 2 achieved three.

The response time of the limiter was experimentally determined using an indirect method. We estimated the time of the exponential decay of the intensity of radiation, transmitted through the sample, provided that the intensity of the incident radiation is constant. Under the used conditions, the response time was 1.0 ± 0.5 ms.

The thermal treatment of Ag_2S QD samples caused an insignificant decrease in the operation threshold, namely, the threshold light flux density changed from 3.1 ± 0.2 and 2.8 ± 0.2 mW cm^{-2} for samples 1 and 2 to 2.6 ± 0.2 and 2.2 ± 0.2 mW cm^{-2} for samples 1′ and 2′, respectively.

An important distinctive feature of thermally treated samples is the absence of clearing even at the maximal values of the incident light flow intensity, which provided a double increase in the dynamical range. Under the actual experimental conditions, the light flow intensities that cause the destruction or clearing of the sample were not attained.

The estimated maximal radiation intensity at the samples located in the focus of the focusing lens (the waist diameter 22 μm, the radiation power 0.23 W) amounts to 60 ± 1 kW cm^{-2}. This value allows one to assume the involvement of real localised states of the Ag_2S QDs in the processes of optical radiation power limiting. Note that in the case of two-photon absorption via virtual states the required intensities are greater than 10 MW cm^{-2} [2, 8, 10, 12, 16, 32, 39, 41]. Since the real localised states are involved in the optical radiation power limiting, the presence of clearing at the pulse energy density 9 ± 0.2 mJ cm^{-2} for samples 1 and 2 is, probably, due to the finite concentration of the impurity centres. In such cases, the concentration of photo-ionised localised states will increase with the growth of the radiation intensity until the majority of them transits into the excited state. A further increase in the incident radiation intensity leads to the clearing of the samples rather than to an increase in their impurity absorption. This feature was mentioned in many publications [5, 17, 37]. Thus, the increase in the dynamic range for the thermally treated samples 1′ and 2′ is apparently due to the growing concentration of localised states (presumably, luminescence centres). The growth of the recombination luminescence intensity in the process of thermal treatment confirms this point of view.

It is important to note that the influence of the Ag_2S QD size on the parameters of the optical radiation power limiting (operation threshold, dynamic range) seems to have no primary importance. When the Ag_2S QD size changes from 1.7 to 3.7 nm, one should expect an increase in the effective cross sections of the light absorption. In this case, the volume-to-surface ratio changes by 2.2 times and we experimentally observe the change in the threshold for power limiting within ±15%. The above facts also evidence in favour of the dominant role of the concentration of localised states in the process of power limiting in Ag_2S QDs.

6. Study of the power limiting mechanism in Ag_2S

The mechanisms responsible for the optical radiation power limiting were studies using the *z*-scanning technique in the closed- and open-aperture regimes (Fig. 5). The pulse energy density (λ = 660 nm) at the sample amounted to 450 J cm^{-2} if the sample was placed into the lens focus (z = 0).

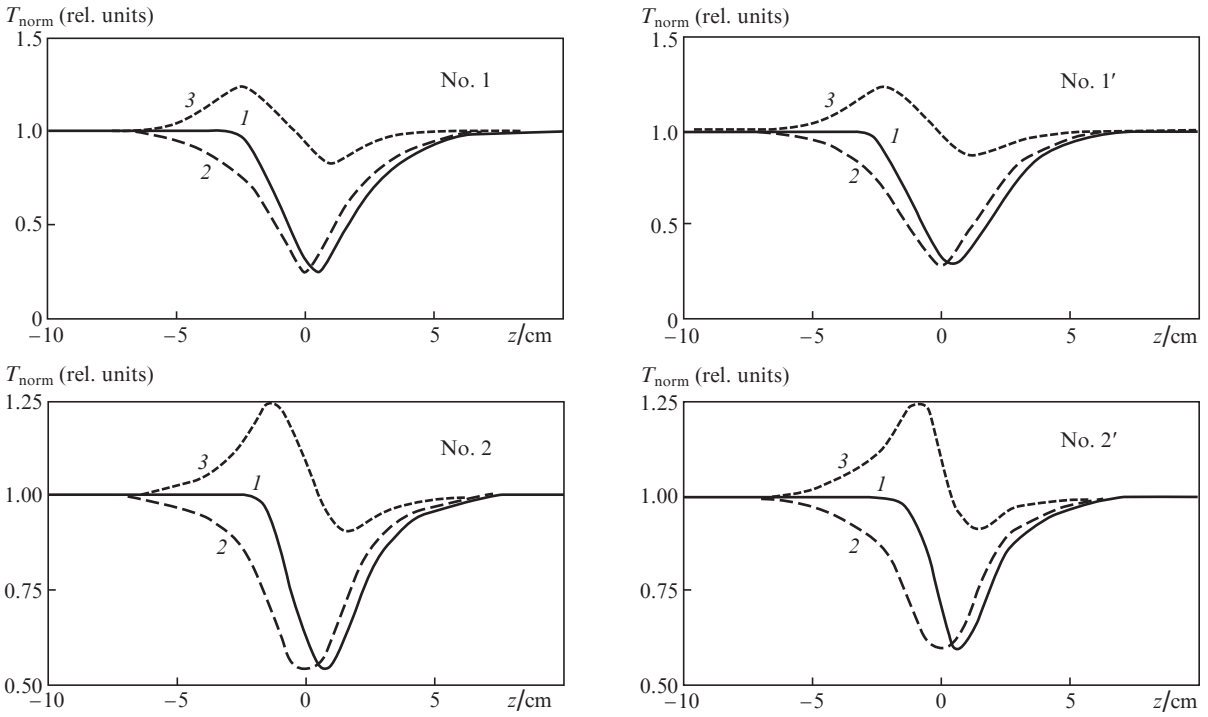

Figure 5. Dependences of normalised transmission on the distance between the samples and the lens focal plane (*z*-scans) for the samples of colloidal Ag_2S QDs in gelatine in the cases of closed (*1*) and open (*2*) apertures; curve (*3*) is the component caused by the self-defocusing.

From Fig. 5 [curves (*1*)] one can see that all experimental *z*-scans, measured in the closed-aperture regime, are asymmetric dependences with a minimum near the lens focal plane. The general view of the *z*-scan dependence, as well as the maximal intensity of radiation at the sample (50 W cm^{-2}) allow the conclusion that the main process is the reverse saturable absorption (RSA) [1, 58], caused by two-quantum transitions in the Ag_2S QD involving the localised states. Moreover, the symmetric shape of the dip in the *z*-scans with respect to the lens focus is a manifestation of nonlinear refraction due to self-defocusing in the sample. In the used geometry the *z*-scan for self-defocusing is an asymmetric curve with respect to $z = 0$ with the maximum for negative *z* values and the minimum for positive ones [Fig. 5, curves (*3*)]. A similar shape of the *z*-scan was demonstrated in Ref. [40] by *z*-scan modelling with the contribution of both two-photon absorption processes and nonlinear refraction taken into account.

To extract the contribution of RSA into the power limitation, we performed the *z*-scan measurements in the open-aperture regime that allowed elimination of the dynamic lens influence on the intensity of the output radiation [Fig. 5, curves (*2*)]. Curves (*3*) were calculated by dividing the dependences of transmission coefficients measured with closed and open apertures. The result presents the contribution to the power limiting determined by self-defocusing.

Let us briefly consider the mechanisms of the dynamic lens formation in the studied samples. The observed nonlinear refraction (self-defocusing) arises due to a decrease in the refractive index under the action of radiation ($\Delta n < 0$). One of the mechanisms of the refractive index variation is due to populating the higher energy states of the Ag_2S QDs via the optical excitation of charge carriers [63, 64]. From the elementary dispersion theory it is known that the refractive index and the concentration of charge carriers are related by the formula $n^2 \propto N$. Therefore, when the concentration of charge carriers at the energy levels of defects in a semiconductor changes, the refractive index also changes. Generally, the refractive index can increase as well as decrease (see, e.g., [32]). This effect is referred to as 'band filling' [64]. The change in the refractive index gives rise to the dynamic lens formation and determines the limiting of the optical radiation power due to nonlinear refraction.

An alternative to the above mechanism of defocusing is the thermal lens. In Ref. [40] it is shown that the nanoparticles of silver sulphide are characterised by the negative temperature coefficient of the refractive index variation dn/dT, equal to -1.17×10^{-4} K^{-1} for the nanoparticles with the mean size 3.0 nm. The dependences [curves (*3*)] in Fig. 5 show the presence of a negative dynamic lens, which is a manifestation of its thermally induced nature.

In the studied colloidal Ag_2S QDs the existence of the inverse-saturation absorption indicates the presence of two-quantum optical transition involving the localised states. This effect is due to the essential difference between the cross sections of the transitions from the size quantisation energy levels to the localised states σ_1 and from the localised states to the size quantisation energy levels of electrons σ_2. According to Ref. [1], in the case of RSA the variation of the intensity of laser radiation propagating through the sample is expressed as

$$dI/dz = -[N_t\sigma_1 + N_2(\sigma_2 - \sigma_1)]I, \quad (1)$$

where *z* is the propagation coordinate; N_t is the number of charge carriers in the initial-state within the layer having the thickness d*z*; and N_2 is the population of the localised states, involved in the two-quantum transitions. If the cross section of the optical transition $\sigma_2 < \sigma_1$, then the second term in expression (1) will be negative, giving rise to an increase in the transmission through the medium (clearing). If, on the contrary, $\sigma_2 > \sigma_1$, then the transmission will decrease with the growth of the population of the localised states [1].

The relation between the population of the excited state N_2 and the total number of defects is determined by several parameters, including the lifetime of the state N_2 and the upper state (the size quantisation state of the electron), as well as the cross sections of the radiation absorption. As seen from Eqn (1) the operation threshold is determined by the condition

$$N_t\sigma_1 \approx N_2(\sigma_2 - \sigma_1). \quad (2)$$

The efficiency of optical limiting, i.e., the reduction of the intensity excess above the threshold, is determined by the ratio σ_2/σ_1. The reduction of the limiting efficiency that occurs in the experiment at the maximal intensities is determined by significant population of the localised states and the upper dimensional quantisation states of the electron, which, in turn, depends on all the parameters mentioned above. The construction of a rigorous mathematical model describing the inverse-saturation absorption in the Ag_2S QDs requires information related to a number of characteristics for the states, involved in its formation, and is a subject of a separate study.

It is worth noting that the high concentration of localised states in samples 1 and 2, playing the role of radiationless recombination centres and capable of capturing a part of charge carriers, can lead to the reduction of the population N_2. If the carrier lifetime at the localised states of the above type is a few microseconds or longer, the decrease in the concentration N_t of carriers in the initial state that participate in two-photon transitions and give rise to RSA is also possible. At power densities of the incident radiation 9–12 mJ cm^{-2} the capture of charge carriers by the radiationless recombination centres not involved in the RSA can lead to the reduction of the limiting efficiency. Within the frameworks of the present work the reduction of the concentration of radiationless recombination centres after the thermal treatment (samples 1′ and 2′) can lead to the growth of the concentration of carriers that take part in two-quantum transitions and, correspondingly, to the elimination of the clearing effect for the energy density 9–12 mJ cm^{-2}, observed in samples 1 and 2.

The study of power limiting and *z*-scans using the laser radiation with $\lambda = 440$ nm and similar power, falling on the exciton adsorption, demonstrated the absence of nonlinear effects.

Thus, the main mechanisms of optical nonlinearity for the Ag_2S QDs are the inverse-saturation absorption involving the localised states and thermally induced nonlinear refraction.

Since there is no generally accepted point of view at the position of the Fermi level in bulk Ag_2S crystals [65–70] and the mechanisms of radiative recombination in Ag_2S QDs [46, 49, 51], the question of whether the luminescence centre is filled with an electron or not before the nanocrystal excitation remains unclear. This fact leads to an uncertainty in the sequence of two-quantum transitions. However, this uncertainty does not affect the possibility of inverse-saturation

scattering and optical radiation power limiting in principle. One should distinguish three basic cases.

1. If the luminescence centre is free of the electron before excitation, then the radiation appears as a result of the recombination of the electron, excited to the luminescence centre, with a hole, occupying the levels of dimensional quantisation (Fig. 6a). Two-quantum transitions involving the energy levels of luminescence centres occur sequentially, first from the quantisation energy levels, filled with electrons, to the luminescence centres, and then from the energy levels of the luminescence centres to the conduction band states. In this case the condition, necessary for the existence of inverse-saturation absorption, is fulfilled if the absorption cross section for the second step σ_2 essentially exceeds the transition cross section for the first step σ_1 that provides the population of the luminescence centres, i.e., $\sigma_2 > \sigma_1$ (Fig. 6a). Then both the radiative and radiationless de-excitation is possible. As a result of radiationless transitions, the energy is dissipated into phonons, which probably gives rise to the thermally induced dynamic lens.

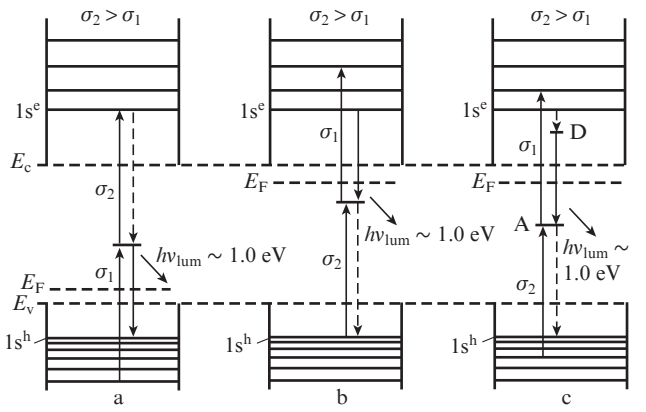

Figure 6. Schematic diagrams of transitions explaining the effect of inverse-saturation absorption; E_F is the Fermi energy; E_c and E_v are the boundaries of the conduction and valence bands in the bulk material, respectively; D and A are the donor and acceptor energy levels.

2. If the luminescence centres are initially occupied with electrons, and the radiation arises as a result of the transition of electrons from the dimensional quantisation states to the luminescence centre (Fig. 6b), then in the course of RSA the first transition will be from the luminescence centre energy levels to the conduction band states with the effective cross section σ_1. The second transition will be from the dimensional quantisation states, populated with electrons, to the luminescence centre with the cross section σ_2. The inverse-saturation absorption is also possible if $\sigma_2 > \sigma_1$.

3. If the emission arises as a result of donor–acceptor recombination, then the transitions in the course of RSA occur as in the second case (Fig. 6c).

7. Conclusion

Thus, we have studied the effect of low-threshold optical power limiting for the radiation with the wavelength 660 nm by the colloidal Ag_2S QDs with the mean size 1.7–3.7 nm, for which the operation threshold amounted to 2.2 ± 0.2–3.1 ± 0.2 mW cm^{-2}, the response time being smaller than 1 ms. Using the *z*-scanning technique in the closed aperture regime it was found that the basic mechanism is the inverse-saturation absorption due to two-photon transitions involving the localised states, i.e. the luminescence centres. The possibility in principle to observe the inverse-saturation absorption does not depend on the mechanisms of recombination luminescence.

Acknowledgements. This work was supported by the Russian Foundation for Basic Research (Grant No. 14-02-31-278 mol_a) and partially supported by the Department of Education, Science and Youth Policy of the Voronezh Region and the Youth Government of the Voronezh Region.

References

1. Tutt L., Boggess T.F. *Progr. Quantum Electron.*, **17**, 299 (1993).
2. Hollins R.C. *Curr. Opin Sol. Mat. Sci.*, **4**, 189 (1999).
3. State Standard R 54838-2011.
4. Wray J.E., Liu K.C., Chen C.H., et al. *Appl. Phys. Lett.*, **64**, 2785 (1994).
5. Mikheev G.M., Kuznetsov V.L., Bulatov D.L., et al. *Kvantovaya Elektron.*, **39**, 342 (2009) [*Quantum Electron.*, **39**, 342 (2009)].
6. Venugopal Rao S., Narayana Rao D., Akkara J.A., et al. *Chem. Phys. Lett.*, **297**, 491 (1998).
7. Wang J., Blau W.J. *J. Opt. A: Pure Appl. Opt.*, **11**, 024001 (2009).
8. Liberman V., Sworin M., Kingsborough R.P., et al. *J. Appl. Phys.*, **113**, 053107 (2013).
9. Sun Y.-P., Riggs J.E., Rollins H.W. *J. Phys. Chem. B*, **103**, 77 (1999).
10. Sun Y.-P., Rings J.E., Henbest K.B., et al. *J. Nonlin. Opt. Phys. Mater.*, **9**, 481 (2000).
11. Muller O., Dengler S., Ritt G., et al. *Appl. Opt.*, **52**, 139 (2013).
12. Martin R.B., Di X., Lei Zh., et al. *Opt. Mater.*, **29**, 788 (2007).
13. Sidorov A.I. *Zh. Tekh. Fiz.*, **76**, 136 (2006) [*Tech. Phys.*, **51**, 477 (2006)].
14. Milichko V.A., Dzyuba V.P., Kul'chin Yu.N. *Kvantovaya Elektron.*, **43**, 567 (2013) [*Quantum Electron.*, **43**, 567 (2013)].
15. Borshch A.A., Starkov V.N., Volkov V.I., et al. *Kvantovaya Elektron.*, **43**, 1122 (2013) [*Quantum Electron.*, **43**, 1122 (2013)].
16. Scalisi A.A., Compagnini G., Urso L., et al. *Appl. Surf. Sci.*, **226**, 237 (2004).
17. Sidorov A.I. *Opt. Zh.*, **69**, 7 (2002) [*J. Opt. Tech.*, **69**, 5 (2002)].
18. Mikheeva O.P., Sidorov A.I. *Opt. Zh.*, **68**, 115 (2001) [*J. Opt. Tech.*, **68**, 278 (2001).
19. Mikheeva O.P., Sidorov A.I. *Zh. Tekh. Fiz.*, **74**, 77 (2004) [*Tech. Phys.*, **49**, 739 (2004)].
20. Baidullayeva A., Vlasenko A.I., Mozol P.E., et al. *Fiz. Tekh. Poluprovodn.*, **38**, 529 (2004) [*Semiconduct.*, **38**, 512 (2004)].
21. Ganeev R.A., Ryasnyanskii A.I., Usmanov T. *Fiz. Tverd. Tela*, **45**, 198 (2003) [*Phys. Solid State*, **45**, 207 (2003)].
22. Bagrov I.V., Zhelvakov A.P., Sidorov A.I. *Pis'ma Zh. Tekh. Fiz.*, **27**, 26 (2001) [*Tech. Phys. Lett.*, **27**, 406 (2001)].
23. Nevejina-Sturhan A., Werhahn O., Siegner U. *Appl. Phys. B*, **74**, 553 (2002).
24. Sharma D., Gaur P., Malik B.P., et al. *Opt. Photon. J.*, **2**, 98 (2012).
25. Smirnov M.S., Ovchinnikov O.V., Novikov P.V., et al. *Opt. Zh.*, **76**, 68 (2009) [*J. Opt. Tech.*, **76**, 725 (2009)].
26. Ovchinnikov O.V., Smirnov M.S., Latyshev A.N., Stasel'ko D.I. *Opt. Spektrosk.*, **103**, 497 (2007) [*Opt. Spectrosc.*, **103**, 482 (2007)].
27. Smirnov M.S., Ovchinnikov O.V., Kosyakova E.A., et al. *Physics B. Condense. Mater.*, **404**, 5013 (2009).
28. Ievlev V.M., Latyshev A.N., Ovchinnikov O.V., et al. *Dokl. Ross. Akad. Nauk*, **409**, 756 (2006) [*Dokl. Phys.*, **51**, 400 (2006)].
29. Ovchinnikov O.V., Vorobyova R.P., Evlev A.B., et al. *Zh. Prikl. Spektrosk.*, **73**, 592 (2006) [*J. Appl. Spectrosc.*, **73**, 662 (2006)].
30. Ovchinnikov O.V., Smirnov M.S., Latyshev A.N., et al. *Kvantovaya Elektron.*, **40**, 490 (2010) [*Quantum Electron.*, **40**, 490 (2010)].
31. Ovchinnikov O.V., Latyshev A.N., Smirnov M.S., et al. *Opt. Spektrosck.*, **114**, 603 (2013) [*Opt. Spectrosc.*, **114**, 554 (2013)].

32. Bolotin I.L., Asunskis D.J., Jawaid A.M., et al. *J. Phys. Chem. C*, **114**, 16257 (2010).
33. Dolotov S.M., Koldunov L.M., Koldunov M.A., et al. *Kvantovaya Elektron*., **42**, 39 (2012) [*Quantum Electron*., **42**, 39 (2012)].
34. Mikheeva O.P., Sidorov A.I. *Pis'ma Zh. Tekh. Fiz*., **30**, 16 (2004) [*Tech. Phys. Lett*., **30**, 223 (2004)].
35. Venkatram N., Narayana Rao D., Akundi M.A. *Opt. Express*, **13**, 867 (2005).
36. Venkatram N., Sai Santosh Kumar R., Narayana Rao D. *J. Appl. Phys*., **100**, 074309 (2006).
37. Kurian P.A., Vijayan C., Sathiyamoorthy K., et al. *Nanoscale Res. Lett*., **2**, 561 (2007).
38. Sahyun M.R.V., Hill S.E., Serpone N., et al. *J. Appl. Phys*., **79**, 8030 (1996).
39. Aleali H., Sarkhosh L., Karimzadeh R., et al. *Phys. Status Solidi B*, **248**, 680 (2011).
40. Karimzadeh R., Aleali H., Mansour N. *Opt. Commun*., **284**, 2370 (2011).
41. Han M.Y., Huaung W., Chew C.H., et al. *J. Phys. Chem. B*, **102**, 1884 (1998).
42. Ouyang Q., Di X., Lei Zh., et al. *Phys. Chem. Chem. Phys*., **15**, 11048 (2013).
43. Dneprovskii V.C., Zhukov E.A., Kozlova M.V., et al. *Fiz. Tverd. Tela*, **52**, 1809 (2010) [*Phys. Solid State*, **52**, 1941 (2010)].
44. Reye H., Schmalzried H. *Zeitschrift fur Physikalische Chemie*, **128**, 93 (1989).
45. Gorbachev V.V. *Poluprovodnikovye soedineniya* (Semiconductor Compounds) (Moscow: Metallurgiya, 1980) p. 12.
46. Ovchinnikov O.V., Smirnov M.S., Shapiro B.I., et al. *Fiz. Tekh. Poluprovodn*., **49**, 385 (2015) [*Semiconduct*., **49**, 373 (2015)].
47. Lin Sh., Feng Y., Wen X., et al. *Phys. Chem. C*, **119**, 867 (2015).
48. Yang H.-Y., Zhao Y.-W., Zhang Zh.-Y., et al. *Nanotechnol*., **24**, 055706 (2013).
49. Peng J., Zhu Ch.-N., Zhang Zh.-L., et al. *Biomater*., **33**, 5130 (2012).
50. Lu X., Li L., Zhang W., Wang C. *Nanotechnol*., **16**, 2233 (2005).
51. Zhang Y., Hong G., Zhang Ye., et al. *ACS Nano*, **6**, 3695 (2012).
52. Chen R., Nuhfer N.T., Moussa L., et al. *Nanotechnol*., **19**, 455604 (2008).
53. Peng J., Zhu Ch.-N., Zhang Zh.-L., et al. *Biomater.*, **33**, 5130 (2012).
54. Wang Ch., Wang Y., Xu L., et al. *Small*, **8**, 3137 (2012).
55. Ovchinnikov O.V., Smirnov M.S., Shapiro B.I., et al. Patent of the Russian Federation No. 2538262 dated 10.01.2015.
56. Vengerovich R.D., Moskalyuk A.V., Yarema S.V. *Fiz. Tverd. Tela*, **49**, 13 (2007) [*Phys. Solid State*, **49**, 11 (2007)].
57. Ovchinnikov O.V., Smirnov M.S., Latyshev A.N., et al. *Teor. Eksp. Khim*., **48**, 48 (2012) [*Theor. Exper. Chem*., **48**, 48 (2012).
58. Sutherland R.I. *Handbook of Nonlinear Optics* (New York: Marcel Dekker Inc., 1996).
59. Van Stryland E.W., Sheik-Bahae M., Said A.A., et al. *Progr. Crystal Growth Charact*., **27**, 279 (1993).
60. Van Stryland E.W., Sheik-Bahae M. *Characterization Techniques and Tabulation for Organic Nonlinear Materials* (New York: Marcel Dekker Inc., 1998) p. 655.
61. Bruhwiller D., Leiggener C., Glaus S., et al. *J. Phys. Chem. B*, **106**, 3770 (2002).
62. Zhang Y., Liu Y., Chen X., et al. *J. Phys. Chem. C*, **118**, 4918 (2014).
63. Hutchings D.C., Sheik-Bahae M., Hagan D.J., et al. *Opt. Quantum Electron*., **24**, 1 (1992).
64. Gilman J.M.A., Hamnett A., Batchelor R.A. *Phys. Rev. B*, **46**, 1363 (1992).
65. Boughalmi R., Boukhachem A., Gaied I., et al. *Mater. Sci. Semicond. Proces*., **16**, 1584 (2013).
66. Jupond P. *Helvetica Phys. Acta*, **32**, 567 (1959).
67. Jadhav U.M., Gosavi S.R., Patel S.N., et al. *Arch. Phys. Res*., **2**, 27 (2011).
68. Grozdanov I. *Appl. Surf. Sci*., **84**, 325 (1995).
69. Wagner C. *J. Chem. Phys*., **21**, 1819 (1953).
70. Nasrallah T.B., Dlala H., Amlouk M., et al. *Synthetic Metals*, **151**, 225 (2005).